

**Binary Star Differential Photometry using the Adaptive Optics system at
Mount Wilson Observatory.¹**

Theo ten Brummelaar ²

Center for High Angular Resolution Astronomy
Georgia State University, Atlanta, Georgia 30303-3083
Electronic mail: theo@mtwilson.edu

Brian D. Mason

U.S. Naval Observatory
3450 Massachusetts Avenue, NW, Washington, DC, 20392-5420
Electronic mail: bdm@draco.usno.navy.mil

Harold A. McAlister ², Lewis C. Roberts Jr. ^{2,3}, Nils H. Turner ^{2,4}, William I. Hartkopf ^{2,5}, and
William G. Bagnuolo Jr. ²

Center for High Angular Resolution Astronomy
Georgia State University, Atlanta, Georgia 30303-3083
Electronic mail: hal@chara.gsu.edu, lroberts@cygnus.mhpcc.af.mil, nils@mtwilson.edu,
hartkopf@chara.gsu.edu, bagnuolo@chara.gsu.edu

¹Based on observations made at Mount Wilson Observatory, operated by the Mount Wilson Institute, under an agreement with the Carnegie Institution in Washington.

²Visiting Astronomer, Mt. Wilson Observatory operated by the Mount Wilson Institute.

³Current address: Rocketdyne Technical Services, 535 Lipoa Pkwy Suite 200, Kihei HI, 96753

⁴Current address: Mount Wilson Institute, Mt. Wilson CA, 91023

⁵Current address: U.S. Naval Observatory, 3450 Massachusetts Avenue, NW, Washington, DC, 20392-5420

ABSTRACT

We present photometric and astrometric results for 36 binary systems observed with the natural guide star adaptive optics system of the Mount Wilson Institute on the Hooker 100-in telescope. The measurements consist of differential photometry in U, B, V, R and I filters along with astrometry of the relative positions of system components. Magnitude differences were combined with absolute photometry found in the literature of the combined light for systems to obtain apparent magnitudes for the individual components at standard bandpasses, which in turn led to color determinations and spectral types. The combination of these results with Hipparcos parallax measurements yielded absolute magnitudes and allowed us to plot the components on an HR diagram. To further examine the reliability and self-consistency of these data, we also estimated system masses from the spectral types.

Subject headings: Adaptive Optics — binaries: general — binaries: visual — binaries: photometry

1. Introduction

While the study of binary star systems is a very mature science, there are relatively few systems for which the temperatures and luminosities of the individual components are known. The Center for High Angular Resolution Astronomy (CHARA) at Georgia State University has been using speckle interferometry for over twenty years to study multiple star systems, and this technique has proved very productive for astrometry. Unfortunately, it has been much less effective in yielding photometric results. For close binary systems it is extremely challenging to obtain accurate photometric measurements of the individual components using standard techniques for, except in exceptional seeing conditions, the images of the two stars overlap. One exception to this statement is the analysis of the Capella system by Bagnuolo & Sowell (1988).

However, adaptive optics makes it feasible to directly measure magnitude differences, and then, by combining these data with photometry of the system as a whole, obtain apparent magnitudes of the individual components. If this is done in a number of filters, colors can be calculated and effective temperatures derived through color-temperature relations. These data can then be combined with parallax measurements to place the stars on an HR diagram.

In 1996 and 1997, CHARA received funding from the National Science Foundation and the Mount Wilson Institute (MWI) to pursue these measurements using the natural guide star adaptive optics system developed by MWI (Shelton et al. 1995) on the Hooker 100-inch telescope. In all, some 36 systems were measured in two or more filters on the Johnson et al. (1966a) system. These results are presented below.

2. Observational and Data Reduction Techniques

The strategy for observation and data reduction was a modification of the methods in our previous work at the Starfire Optical Range (SOR) by ten Brummelaar et al. (1996). A relatively short exposure time was chosen such that the image was not saturated, but the signal was well above the bias levels of the CCD camera. Between 10 and 50 exposures were taken of the object and then integrated into a composite image using a shift-and-add algorithm in which the Strehl ratio serves as a weight for each frame.

We then assume that the image consists of a series of functions of the form

$$\delta(x, y) = \begin{cases} 1 & \text{for } x = 0 \text{ and } y = 0 \\ 0 & \text{otherwise.} \end{cases} \quad (1)$$

So if the intensity of the i th star is A_i and its position is (x_i, y_i) the ‘clean’ image can be written

$$I(x, y) = \sum_{i=1}^N A_i \delta(x - x_i, y - y_i). \quad (2)$$

This image must then be convolved with the PSF $P(x, y)$ to yield the ‘dirty’ image

$$O(x, y) = I(x, y) * P(x, y), \quad (3)$$

where we assume that the PSF does not change over the small 2 arcsecond field.

Given that you have a pixel by pixel model of the PSF, which in the first instance can be provided by an image of a single star, one can then solve, in a least squares sense, for the position and magnitudes of the stars in the field. Of course, it is well known that an image of a single star does not make a very good PSF model since both the performance of the AO system and the atmosphere itself will change substantially between observations. Thus, with these estimates of position and magnitude one extracts a new model of the PSF from the data itself using

$$P_k(x, y) = O(x, y) - \sum_{j \neq i} A_j (\delta(x - x_j, y - y_j) * P_{k-1}(x, y)), \quad (4)$$

which can be done for each star in the field and a mean, weighted by magnitude, created. This is a new PSF model and the process can be repeated until the results converge.

There are two areas in which our current techniques differ from those used in our earlier SOR work. The first is in the way we prevent the solution from converging to a single delta function and a multiple PSF model, which is a mathematically valid solution but not a useful one. Unless we are very close to convergence, the PSF model often contains some energy at the positions of the fainter stars in the field. In our previous work we forced the PSF model to exist only within a predefined boundary and to be zero elsewhere. This method ignores the often large amount of energy in the PSF wings. Instead of forcing the wings to zero, we now force the PSF to be circularly symmetric in the wings. Thus the PSF model has a non-analytical part consisting of

a matrix of numbers near the center, and a series of single values for various distances from the center. We found that a cross-over point based on the first estimate of magnitude distance worked well, that is

$$r_{\text{cross}} = \sqrt{(x_1 - x_2)^2 + (y_1 - y_2)^2} \times \frac{A_1}{A_1 + A_2}. \quad (5)$$

In some cases it was necessary to manually manipulate this cross-over point in order to find the solution with the lowest residuals.

The second way in which we have changed our reduction method is in the area of error estimation. We now believe that the errors of the original work at SOR were underestimated and represent a lower bound on the errors. This is because those errors were based directly on the formal errors that came out of the least squares fitting process. Since this is only valid if the functional form of the PSF is known exactly, which can never truly be the case, this will not be a true representation of the errors of the results. Simply using the formal error of the fit does not include the errors in the PSF model itself.

We now base our errors on a series of experiments in which we created a large pool of simulated data of known separation and magnitude difference, and applied our reduction software to these images. We collected data on some 74 stars, known to be single within the resolving power of the telescope, in exactly the same way as we did for the binary systems. We then normalized these images to form PSF models and used equations 2 and 3 to create an ensemble of model binary star images ranging from 0 to 7 in magnitude difference and up to 2 arcseconds in separation. All in all this represented a pool of over 30,000 model images. We then ran our reduction software on these data.

The resulting errors are a function of the magnitude difference and the separation, expressed in terms of the FWHM of the PSF. We found that one could reach the 10% level at small separations (a few FWHMs) down to a magnitude difference of 2, while if the stars are well separated one can reach 5.5 magnitudes. The 1% error level can reach as deep as 3 magnitudes, while you can go as deep as 7.5 magnitudes at the 15% level. The errors are a strong function of how well the AO system is performing, which is in turn a function of the current seeing conditions. Since we did not have the luxury of working only in good seeing, which was on occasion in excess of 2 arcseconds, we were forced to use what data we could collect. If the AO system is performing at the diffraction limit, which is not always the case in the V or B bands, one is often operating in the 1 to 2% regime. At other times the errors will be larger, depending on the FWHM yielded by the system. One would expect much smaller errors in an infrared AO system.

This method of estimating errors is much more conservative than those used in the past, including by us, as it does more than quote the formal error of the least squares fitting process. We believe it to be closer to an upper bound. This should be taken into account when comparing the results from the two sets of measurements. These methods are more fully described in ten Brummelaar et al. (1998) and Roberts (1998).

The deconvolution routine provided a measurement of the differential magnitude of the two stars along with differential astrometric results which we transform into the standard (θ, ρ) system for binary star measurements. The astrometry was calibrated with contemporaneous speckle interferometry measurements obtained on the 100-in telescope (Hartkopf et al. 1999). The results are given in tables 1 and 2. In Table 1, the first five columns give various identifications: the Washington Double Star (WDS) Catalog coordinate (Worley & Douglass 1997), the discovery designation (as defined in the WDS), HR and HD numbers, and the Bayer or Flamsteed designation. For subsequent tables, only the WDS coordinate is used, so Table 1 also serves as a cross reference for the other Tables. Columns 6–8 of Table 1 provide the basic calibrated astrometric data: time (expressed in fractional Besselian year), position angle θ (measured for the secondary relative to the primary from north to east in degrees), and angular separation ρ (in seconds of arc). The last three columns in Table 1 give residuals to the orbit referenced in the final column.

While astrometry was not the primary objective of these data (speckle interferometric techniques provide more accurate and more straightforward measurements of θ and ρ), the astrometric results do provide a good check on the orbital parameters of these systems. However, in comparison with the autocorrelation methods commonly used with speckle interferometry, AO yields a direct image of a system. Thus, the 180° uncertainty in position angle, inherent in earlier reductions of speckle interferometric data, is avoided. While current reduction techniques (i.e., the DVA algorithm, see Bagnuolo et al. 1992) can avoid this ambiguity, AO is more sensitive to very small magnitude differences. In the case of four systems, the correct quadrant identification indicated the published orbital analyses had the longitude of periastron (ω) off by 180° . Those systems are flagged by the letter “r” adjacent to the $\Delta\theta$ residual in column 9 of Table 1. In all cases, the determined astrophysical parameters of these systems are unchanged by the alteration of ω . In large angle astrometry the photocenter of these systems (which would probably be unresolved) would be determined for the wrong quadrant leading to a position error. In three of these cases, the small Δm was responsible for the incorrect assignment of ω , and any consequential photocenter shift would be negligible. In the case of FIN 328, an incorrect quadrant was assigned by speckle interferometry leading to the error [the quadrant was identified correctly by Finsen (1956) and noted by Soderhjelm (1999)].

Table 2 provides the raw differential photometry for each observation. Column 1 lists the WDS coordinate while column 2 provides the date of observation. Columns 3–7 give the differential magnitude and error estimate for each system in the indicated passband. Most objects have magnitude differences in three to four passbands. Only one observation provides all five colors, while two observations provide only two colors.

The U and B filters were not always available, and in some cases the deconvolution did not converge. These factors result in the omissions from Table 2. In other cases, we measured an object twice on different epochs in order to test the consistency of the methods used. Except in the shorter wavelengths where the performance of the AO system was poor, these data are entirely self

consistent giving us confidence in the results. Even in the bluer bands the multiple measurements are very close, and, at worst, indicate that our error bars are underestimated in this band.

In order to evaluate the quality of our measurements, a literature search was done to find existing Δm values, which we present in Table 3. In this table, the same WDS Catalog coordinate identification is used. The literature sources of Δm are the Hipparcos Catalogue (ESA 1997), the WDS catalog (Worley & Douglass 1997), and the USNO Δm Catalog. Many double star lists do not provide true measures of Δm , but simply repeat values from other catalogs. Consequently, the WDS Δm provides only a gross estimate and should be given the lowest weight. The internal USNO Δm catalog was initially assembled by Charles Worley to include only those measures of differential magnitude known to be original. The USNO is currently preparing a new WDS which will include the Δm catalog and incorporate multi-dimensional weighting of data to provide a more accurate representation of Δm (for further information, see <http://aries.usno.navy.mil/ad/wds/wds.html>).

Although not widely noted, many clever and useful approaches to measuring Δm ’s were developed prior to the modern generation of techniques based upon digital detectors. These methods generally provided measurements freer of subjective bias than simple visual estimates of Δm and include such techniques as: double image photometry (Pickering 1879, Stebbins 1907, Wendell 1913), wedge photometry (Wallenquist 1947, Pettit 1958, Rakos et al. 1982), objective gratings (Baize 1950), double image micrometry (Muller 1952, van Herk 1966, Worley 1969), and area scanning (Rakos et al. 1982, Franz 1982).

The above methods are generally no longer practiced, and no methods of even comparable reliability have come along to replace them in any systematic fashion. Speckle interferometry offers the potential for extracting differential photometric information from speckle images, but the actual practice of this is not straightforward. In many cases, speckle data are obtained with non-linear image intensifiers often yielding saturated images. Calibration for atmospherically induced biases in speckle data is also a non-trivial task. Perhaps the best speckle photometric analysis is that of Bagnuolo & Sowell (1988) for the components of Capella. However, the overall brightness and near-zero Δm of that system make it an ideal candidate for careful speckle analysis. Dombrowski (1991) measured Δm ’s in V for Hyades binaries using the “fork” algorithm of Bagnuolo (1988) applied to speckle data and found $\Delta m = 0.19$ for WDS 04512+1104, in satisfactory agreement with our value of $\Delta m = 0.15 \pm 0.04$. Ismailov (1992) fit visibility curves from speckle data obtained at 500 nm. Seven of our systems were also measured by Ismailov, and in comparing our results with his in the sense of AO-speckle, we find a dispersion of ± 0.76 magnitudes indicative of poor agreement with Ismailov’s differential photometry.

The Δm measurements of Hipparcos are plotted against our V band measurements in Figure 1. Even though the Hipparcos photometric band H_p is broader and peaks blueward in comparison with the standard Johnson V used with the Mt. Wilson AO system, Figure 1 clearly shows that our measurements are consistent with those of Hipparcos, with the errors increasing with increasing

Δm as one would expect. For small Δm objects the match between our data and those of Hipparcos is excellent. From residuals defined in the sense AO–Hipparcos, we find a mean residual and rms dispersion of $+0.03 \pm 0.15$ magnitudes, improving to $+0.01 \pm 0.10$ magnitudes when we omit systems for which we calculate $\Delta m \geq 2.0$ magnitudes. We find no obvious correlation between spectral type of the primary component and the AO–Hipparcos residual, although most of our stars are confined to systems of intermediate spectral types. A similar comparison in AO–WDS magnitudes yields a mean and standard deviation of $+0.06 \pm 0.35$ magnitudes with no significant improvement resulting from including only systems with smaller Δm ’s.

Another test of the accuracy of our AO photometry is obtained by comparing our new results with photometry from another AO system. Thus, we note that the R-band Δm for WDS 20375+1436 measured at SOR (ten Brummelaar et al. 1996) was 1.04 ± 0.01 while our new measurements on two nights at Mt. Wilson are 0.93 ± 0.11 and 1.03 ± 0.08 . As discussed above, we now believe that the errors given for the SOR measures are underestimated. Furthermore, the filters used at SOR were not standard astronomical filters. Nevertheless, the two measures at Mt. Wilson are entirely consistent with the earlier SOR measurement. Unfortunately, this is the only system we have in common with our earlier SOR results. Similarly, we note that the Δm at V of 1.67 ± 0.72 magnitudes measured from lunar occultation data for WDS 21044–1951 by Evans & Edwards (1983) is within one standard deviation of our value of 2.18 ± 0.22 .

As a final test, different measures of the same system on different nights, while of variable quality, show that the methodology used produces repeatable results. Nine systems in Table 2 were measured on successive nights. Inspection of the pairs of measurements of Δm in V, R, and I show mean dispersions of ± 0.051 , ± 0.041 , and ± 0.046 magnitudes at those passbands. These comparisons lend confidence in a level of precision of ± 0.05 magnitudes. Because we find no evidence for any systematic differences between our differential photometry and that from the Hipparcos mission, we suggest that this level of internal consistency is also indicative of the accuracy of our measurements.

3. Absolute Photometry

Differential magnitudes must be combined with a system’s composite photometry of the systems as a whole in order to obtain apparent magnitudes of the individual components using the equations

$$m_A = m + 2.5 \log \left(1 + 10^{-0.4\Delta m} \right) \quad (6)$$

and

$$m_B = m_A + \Delta m. \quad (7)$$

The General Catalogue of Photometric Data (Mermilliod et al. 1997) provides a comprehensive listing of the composite photometric data on most of the systems we measured. Few of these records provided error estimates, so they were assumed to be ± 0.02 magnitudes in all cases. For the objects for which we could not find literature values, we were forced to use our own data to provide combined magnitudes. The data were reprocessed using a shift-and-add routine that weighted each frame equally and normalized the intensities to a one-second exposure. The total intensity of each system was then calibrated against the literature values to obtain combined magnitudes. Figure 2 is a plot of our calibrated measures of total magnitudes against the literature values in the R band. Other bands produced similar results, and our final apparent magnitude results are given in Table 4, with those based on our photometry marked with an asterisk. The systems in Table 4 are identified by their WDS coordinate in Column 1. Columns 2–9 provide the deconvolved magnitudes of the components. These data allow us to calculate the colors presented in Table 5 in which column 1 provides the WDS coordinate and columns 2–7 present the colors (B–V, V–R, and R–I) colors for the components. Table 6 contains absolute magnitudes for the individual components based on parallax results from Hipparcos (ESA 1997) and the apparent magnitudes in Table 4. Column headings are self evident.

4. Spectral Types and Derived Parameters

With colors and absolute magnitudes it is now possible to assign spectral types, effective temperatures and absolute bolometric magnitudes to the individual components of the systems we have observed. These results are shown in Table 7. The first two columns of Table 7 give the WDS designation and the spectral type listed in the WDS. The third column gives the composite spectral types of Christie & Walker (1969) or Edwards (1976). The magnitudes from Table 6 were used to generate three colors for which spectral types, and ranges were calculated using the tables of Johnson (1966). These results are given in columns 4–6 of Table 7. In each case, the table appropriate for the luminosity class of the WDS type was used, except in the few cases where the color difference was outside the values covered by that table. These systems are marked by notes in Table 7. A fourth measure of the spectral type, listed in column 7, was obtained by using the absolute magnitude from Table 6 and the tables of stellar temperatures and luminosity compiled by Landolt-Börnstein (1980). The final assignment and range of spectral type was given to each object by an averaging process, with the most weight being given to those measurements with color differences with smallest range, and the least weight being given to the estimate based on absolute magnitude. The assigned spectral types resulting from our data are given in the last column of Table 7.

In most cases, especially those with the best color determinations, all four spectral type derivations gave very consistent results. For those systems that did not have self-consistent results, the error bars on the color differences were either large, or the system is not a simple binary.

When we compare our spectral types with those listed in the second and third columns

of Table 7, we find no evidence for any systematic differences and find an rms dispersion of approximately 2.3 subclasses in comparing our results with those taken from the literature. We exclude the two late O-type systems WDS 20035+3601 and 20181+4044 in this evaluation, noting that these systems are known to have a third component not resolved in our measurements.

We use the assigned spectral types from Table 7 to derive astrophysical parameters for the individual components which we present in Table 8. We repeat the WDS designation and assigned spectral type in the first two columns of Table 8. Column 3 contains T_{eff} values from Landolt-Börnstein (1980) corresponding to our spectral types with errors based upon the range in the assigned type. Bolometric corrections taken from the same source were then used to calculate absolute bolometric magnitudes (using our absolute magnitudes in Table 6) which are recorded in column 4.

We also include in Table 8 information about the total mass for most of the systems we have observed. Söderhjelm (1999) calculated systemic masses for binaries for which reliable parallaxes were determined by Hipparcos, and we include his results for 15 systems in column 5 of Table 8. He calculated formal errors incorporating parallax error and uncertainties in the values of the orbital period and semi-major axis, and we include his error estimates in column 5. We have calculated mass sums for seven additional systems not considered by Söderhjelm but similarly based upon Hipparcos parallaxes and published orbital elements. We have not calculated error estimates for these mass sums because the adopted orbits we have taken from the literature did not present formal errors for the elements P and a . Thus our “orbital” mass estimates in Table 8 are distinct from those of Söderhjelm (who calculated orbital elements himself directly from published visual or speckle observations) in the absence of error estimates. The final column in Table 8 gives an estimate of the total mass based upon the spectral types we have assigned to the individual components. The corresponding masses are taken from the tables of Allen (1973). We flag with an asterisk those systems thought or known to be at least triple in multiplicity. In general, there are no surprises resulting from a comparison of the “orbital” and “spectroscopic” masses.

Given the effective temperatures and bolometric magnitudes, it is possible to plot the systems on the HR diagram of Figure 3, in which the primary and secondary of each system are joined by a dotted line and error bars are shown for each component. As one might expect from our inherent sensitivity to modest Δm ’s, in most systems the primary and secondary do not fall very far apart on the HR diagram due to coevolutionary origins. Four systems exhibit post-main sequence evolution of the more massive component. For one of these, WDS 19307+2758, our data were very poor. The $V - R$ type did not differ very much from the WDS designation and the V designations were off scale. We therefore chose to accept the WDS types for the components, so this is not a new result. The other three; WDS 04139+0916, 06573+5825, and 20181+4044 have one component on the main sequence and the other component highly evolved.

5. Conclusion

Magnitudes and colors have been presented for the components of 36 binary star systems. Comparison with Δm measurements from the literature and examination of the HR diagram and spectroscopic masses for these components demonstrates the reliability and self-consistency of these results. Thus, despite our early misgivings about the precision of adaptive optics measurements of close binaries, we have shown that it is possible to get good photometric results with an AO system. Four systems among those presented here appear to contain a highly evolved companion and deserve follow-up observation. Spectrographic data on these systems will be obtained in the near future in order to try and confirm these findings. Now that the reduction techniques have been developed, we hope that similar measurements will continue to be made, and we note the potentially valuable contribution AO observations can make when applied to systems with an intrinsically variable component.

We thank the staff of the Mount Wilson Institute for their help in making this work possible. CHARA's adaptive optics research has been supported by the National Science Foundation, most recently through grants AST-94-21259 and AST-94-23744, the Mount Wilson Institute, and the Research Program Enhancement Fund at Georgia State University. Research with the adaptive optics system on mount Wilson has also been supported by the Max Kampelman Fellowship fund, the Ahmanson Foundation, the Fletcher Jones Foundation and the Parsons Foundation.

REFERENCES

- Allen, C.W. 1973, *Astrophysical Quantities* (Univ. of London, London)
- Bagnuolo, W.G. 1988, *Opt. L.*, 13, 997
- Bagnuolo, W.G. & Sowell, J. 1988, *AJ*, 96, 1056
- Bagnuolo, Jr., W.G., Mason, B.D., Barry, D.J., Hartkopf, W.I., & McAlister, H.A. 1992, *AJ*, 103, 1399
- Baize, P. 1950, *J. Observateurs*, 33, 1
- Baize, P. 1980, *A&AS*, 39, 83
- Baize, P. 1993, *A&AS*, 99, 205
- Finsen, W.S. 1956, *Union Obs. Circ.*, 6, 259
- Landolt-Börnstein, Ed: K.H. Hellwege, Spring-Verlag, Berlin, 1980
- ten Brummelaar, T.A., Mason, B.D. Bagnuolo, Jr., W.G., Hartkopf, W.I., McAlister, H.A. & Turner, N.H. 1996, *AJ*, 112, 1180
- ten Brummelaar, T.A., Hartkopf, W.I., Mason, B.D., McAlister H.A., L.C. Roberts Jr., L.C. & Turner, N.H. 1998, *Proc SPIE*, 3353, 391
- Cester, B. 1991, *Circ. Inf. No.* 113
- Christy, J.W., Walker, Jr., R.L. 1969, *PASP*, 81, 643
- Docobo, J.A., & Costa, J.A. 1987, *Circ. Inf. No.* 102
- Docobo, J.A., & Ling, J.F. 1997, *Circ. Inf. No.* 133
- Docobo, J.A., & Ling, J.F. 1999, *ApJS*, 120, 41
- Dombrowski, E.G. 1991, Ph.D. thesis, Georgia State University
- Edwards, T.W. 1976, *AJ*, 81, 245
- ESA, 1997, *The Hipparcos and Tycho Catalogues* (ESA SP-1200) (Noordwijk: ESA)
- Evans, D.S. & Edwards, D.A. 1983, *AJ*, 88, 1845
- Fekel, F.C., Scarfe, C.D., Barlow, D.J., Duquenooy, A., McAlister, H.A., Hartkopf, W.I., Mason, B.D., & Tokovinin, A.A. 1997, *AJ*, 113, 1095
- Finzi, C. & Giannuzzi, M. 1955, *Oss. Astron. Monte Mario Cont.*, 222
- Franz, O.G. 1982, private communication.
- Hall, R.G. 1949, *AJ*, 54, 102
- Hartkopf, W.I. et al. 1999, (*in progress*)
- Hartkopf, W.I., Mason, B.D., & McAlister, H.A. 1996, *AJ*, 111, 370
- Hartkopf, W.I., McAlister, H.A., & Franz, O.G. 1989, *AJ*, 98, 1014

- Heintz, W.D. 1965, Veroff. Sternw. Munchen, 7, 7
- Heintz, W.D. 1970, AJ, 75, 848
- Heintz, W.D. 1984, A&AS, 56, 5
- Heintz, W.D. 1995, ApJS, 99, 693
- Heintz, W.D. 1997, A&AS, 111, 335
- van Herk, G. 1966, J. Observateurs, 49, 355
- Ismailov, R.M. 1992, A&AS, 96, 375
- Johnson, H.L., Mitchell, R.I., Iriarte, B., & Wisniewski, W.Z. 1996, Comm. Lunar & Planet. Lab., 4, 99
- Johnson, H.L., A.R.A.A 1966, 4, 193
- Mason, B.D., Douglass, G.G., & Hartkopf, W.I. 1999, AJ, 117, 1023
- Mason, B.D., McAlister, H.A., Hartkopf, W.I., & Bagnuolo, Jr. W.G. 1993, AJ, 105, 220
- Mason, B.D. McAlister, H.A., Hartkopf, W.I., & Shara, M.M. 1995, AJ, 109, 332
- Mermilliod, J.-C., Hauck, B, & Mermilliod, M. 1997, A&AS 124, 349,
<http://obswww.unige.ch/gcpd/gcpd.html>
- Muller, P. 1952, Ann. Obs. Strasbourg, 5, Pt. 4
- Pettit, E. 1958, AJ, 63, 324
- Pickering, E. 1879, Harvard Annals, 11, 105
- Rakos, K. et al. 1982, Inst. of Astron. Wien
- Roberts Jr. L.C., 1998, PhD thesis, Georgia State University
- Shelton, J.C., Schneider, T., McKenna, D. & Baliunas, S.L. 1995, Proc. SPIE, 2534, 72
- Söderhjelm, S. 1999, A&A, 341, 121
- Starikova, G.A. 1985, Trud. Astron. Inst. Sternberg, 57, 243
- Stebbins, J. 1907, Univ. Illinois, Studies, II, No. 5
- Wallenquist, A. 1947, Ann. Uppsala Astron. Obs., 2, No. 2
- Wendell, D. 1913, Harvard Annals, 69, 180
- Wierzbinski, S. 1956, Acta Astron., 6, 82
- Worley, C.E. 1969, AJ, 74, 764
- Worley, C.E. & Douglass, G.G. 1997, A&AS, 125, 523,
<http://aries.usno.navy.mil/ad/wds/wdsold.html>
- Zulevic, D.J. 1988, Circ. Inf. No. 106

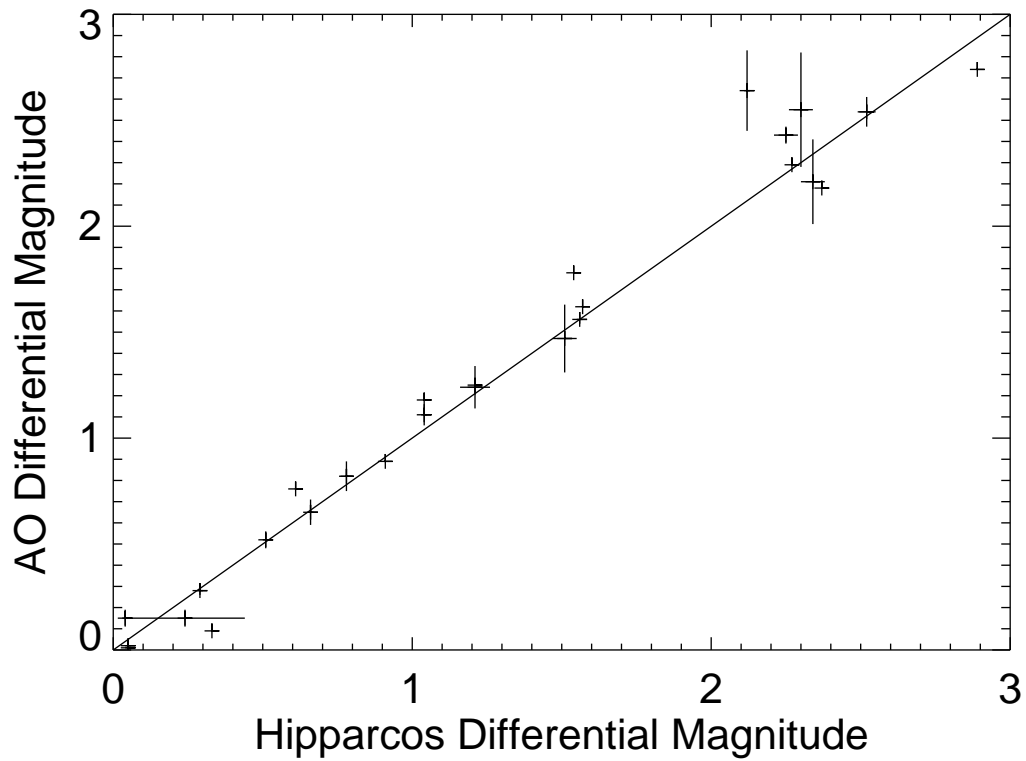


Fig. 1.— Comparison of Hipparcos measures of differential magnitude with the measures made on the Mount Wilson 100-in AO system.

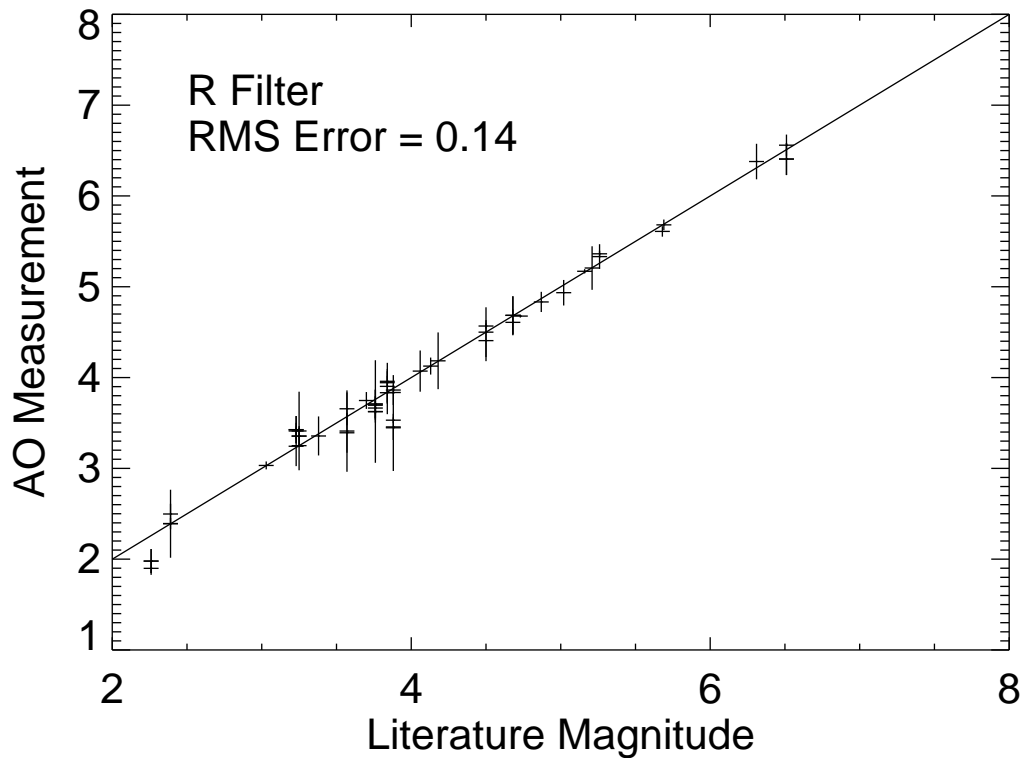


Fig. 2.— An example of the photometric results, with the total photometry as measured by the AO system compared to the values found in the literature.

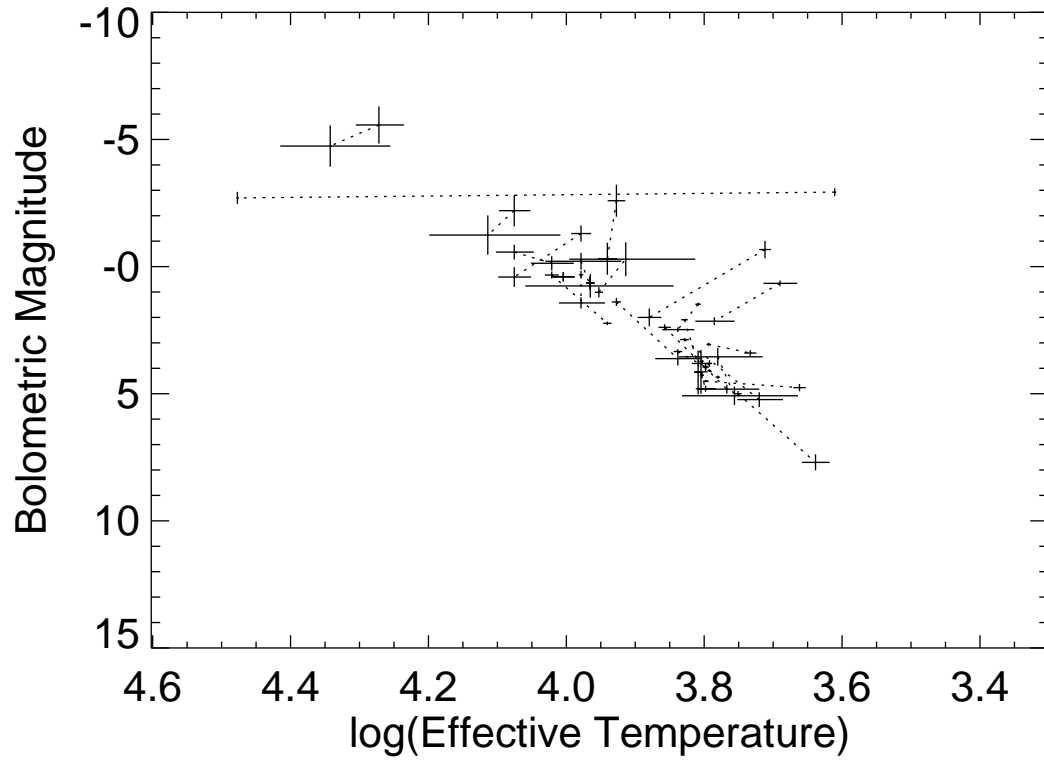


Fig. 3.— HR diagram of all systems measured. The dotted lines connect primary and secondary on each system.

Table 1. AO Astrometry

WDS or α, δ (2000)	Discovery Designation		HR	HD	Name	BY 1990.+	θ ($^{\circ}$)	ρ ($''$)	$\Delta\theta$ ($^{\circ}$)	$\Delta\rho$ ($''$)	Orbit Ref.	
00022+2705	Bu	733	AB	9088	224930	85 Peg	6.7842	151	0.76	-1	+0.02	Hall (1949)
00318+5431	Stt	12		123	2772	λ Cas	6.7843	194	0.42	+0	-0.04	Heintz (1995)
02140+4729	StF	228		647	13594		6.7845	280	1.03	+1	-0.01	Heintz (1984)
04139+0916	Bu	547	AB	1311	26722	47 Tau	6.7818	342	1.24			
04239+0928	Hu	304		1381	27820	66 Tau	6.7900	335	0.11	+8	-0.01	Starikova (1985)
04301+1538	StF	554		1422	28485	80 Tau	6.7847	18	1.61	+1	-0.12	Baize (1980)
							6.7901	17	1.63	+0	-0.10	
04382-1418	Kui	18		1481	29503	53 Eri	6.7847	350	0.92	+0	-0.05	Hartkopf et al. (1996)
04512+1104	Bu	883	AB	—	30810		6.7901	225	0.27	-1 r	-0.01	Heintz (1969)
05387-0236	Bu	1032	AB	1931	37468	σ Ori	6.7901	121	0.26	+1	+0.01	Hartkopf et al. (1996)
05413+1632	Bu	1007		1946	37711	126 Tau	6.7902	244	0.29	+2	-0.01	Docobo & Ling (1999)
06573+5825	Stt	159	AB	2560	50522	15 Lyn	6.7902	216	0.30	-10	-0.02	Baize (1993)
09006+4147	Kui	37	AB	3579	76943		7.2820	89	0.43	+1	+0.00	Hartkopf et al. (1996)
11182+3132	StF	1523	AB	4374/5	98230/1	ξ UMa	7.2794	291	1.54	-2	+0.01	Mason et al. (1995)
							7.2823	291	1.52	-2	-0.01	
13099-0532	McA	38	Aa	4963	114330	θ Vir	6.5019	336	0.45			
13100+1732	StF	1728	AB	4968/9	114378/9	α Com	6.5019	192	0.33	+0 r	+0.00	Hartkopf et al. (1996)
14411+1344	StF	1865	AB	5477/8	129246/7	ζ Boo	6.4992	122	0.82	+1 r	-0.05	Wierzbinski (1956)
							7.2826	121	0.83	+0 r	-0.02	
15038+4739	StF	1909		5618	133640	44 Boo	7.2798	50	1.97	-2	-0.09	Heintz (1997)
15183+2650	StF	1932	Aa-B	—	136176		7.6052	256	1.56	-2	-0.03	Heintz (1965)
15232+3017	StF	1937	AB	5727/8	137107/8	η CrB	6.4965	47	0.90	+0	-0.01	Mason et al. (1999)
							7.6025	51	0.87	-1	+0.01	
15427+2618	StF	1967		5849	140436	γ CrB	6.4965	117	0.68	+1	-0.01	Hartkopf et al. (1989)
							7.2828	113	0.71	-2	+0.00	
16309+0159	StF	2055	AB	6149	148857	λ Oph	6.4939	26	1.37	-1	-0.15	Finzi & Giannunzzi (1955)
							7.2830	24	1.39	-4	-0.13	
17104-1544	Bu	1118	AB	6378	155125	η Oph	6.4967	245	0.51	+0	-0.01	Docobo & Ling (1997)
							6.5021	246	0.51	+1	-0.01	
19307+2758	McA	55	Aa	7417	183915	β^1 Cyg	6.4995	139	0.39			
19553-0644	StF	2597		7599	188405		6.4996	105	0.38	+0	+0.00	Hartkopf et al. (1996)
							7.6001	117	0.37	+12	-0.04	
20035+3601	StF	2624	Aa-B	—	190429		6.4997	174	1.95			
20181+4044	StF	2666	Aa-B	7767	193322		6.4970	245	2.71			
20203+3924	A	1427	AB	7784	193702		6.4970	117	0.34	+1	+0.03	Docoba & Costa (1987)
20375+1436	Bu	151	AB	7882	196524	β Del	6.4942	315	0.32	+0	+0.02	Hartkopf et al. (1989)
							6.4998	317	0.32	+2	+0.02	
21044-1951	Fin	328		8060	200499	η Cap	6.4998	236	0.26	+1 r	-0.01	Mason et al. (1999)
21145+1000	Stt	535	AB	8123	202275	δ Equ	6.4944	20	0.27	+1	+0.00	Hartkopf et al. (1996)
21148+3803	AGC	13	AB	8130	202444	τ Cyg	6.4944	327	0.80	-2	+0.03	Heintz (1970)
21186+1134	Bu	163	AB	—	202908		6.4999	262	0.42	+0	-0.02	Fekel et al. (1997)
21441+2845	StF	2822	AB	8309	206826/7	μ Cyg	6.7811	305	1.92	+1	+0.02	Heintz (1995)
21501+1717	Cou	14		8344	207652	13 Peg	6.4945	233	0.38	-1	+0.00	Hartkopf et al. (1989)
22300+0426	StF	2912		8566	213235	37 Peg	6.4945	116	0.48	-2	-0.02	Zulevic (1988)
22586+0921	Stt	536	AB	8737	217166		6.4972	349	0.19	+2	-0.12	Cester (1991)

Table 2. AO Differential Photometry

WDS or α, δ (2000)	BY 1990.+	U Δm	B Δm	V Δm	R Δm	I Δm
00022+2705	6.7842			3.08±0.29	2.70±0.27	2.35±0.26
00318+5431	6.7843			0.15 0.04	0.10 0.04	0.13 0.04
02140+4729	6.7845			0.65 0.06	0.59 0.04	0.54 0.02
04139+0916	6.7818			2.43 0.04	2.86 0.07	3.28 0.13
04239+0928	6.7900			0.90 0.12	0.97 0.11	0.21 0.04
04301+1538	6.7847			2.35 0.20	2.19 0.17	2.02 0.12
	6.7901			2.54 0.07	2.37 0.05	2.21 0.03
04382–1418	6.7847				2.39 0.23	3.02 0.20
04512+1104	6.7901			0.15 0.04	0.18 0.04	0.20 0.04
05387–0236	6.7901			1.24 0.10	1.34 0.13	1.25 0.15
05413+1632	6.7902			1.47 0.16	1.51 0.18	1.52 0.18
06573+5825	6.7902			1.16 0.11	1.41 0.08	1.60 0.18
09006+4147	7.2820	2.11±0.22		2.55 0.27	2.19 0.15	2.06 0.23
11182+3132	7.2794		0.62±0.08	0.53 0.09	0.47 0.06	0.40 0.04
	7.2823		0.47 0.05	0.42 0.06	0.28 0.06	0.18 0.04
13099–0532	6.5019		2.11 0.23	2.21 0.20	2.08 0.20	2.16 0.21
13100+1732	6.5019		0.04 0.04	–0.01 0.06	0.00 0.04	0.00 0.03
14411+1344	6.4992		–0.00 0.02	0.02 0.01	0.01 0.01	0.02 0.01
	7.2826	0.06 0.02	–0.02 0.09	0.07 0.04	0.01 0.03	0.05 0.03
15038+4739	7.2798		1.28 0.16	0.82 0.07	0.61 0.03	0.52 0.04
15183+2650	7.6052		0.02 0.04	0.01 0.03	0.00 0.04	–0.03 0.10
15232+3017	6.4965		0.32 0.02	0.28 0.02	0.26 0.01	0.25 0.01
	7.6025		0.36 0.06	0.29 0.06	0.28 0.04	0.25 0.04
15427+2618	6.4965		1.69 0.08	1.56 0.02	1.43 0.02	1.33 0.03
	7.2828		1.85 0.11	1.59 0.12	1.41 0.06	1.28 0.06
16309+0159	6.4939			1.07 0.14	1.03 0.04	1.02 0.03
	7.2830		1.12 0.07	1.11 0.05	1.09 0.05	1.06 0.03
17104–1544	6.4967		0.50 0.06	0.52 0.04	0.53 0.03	0.53 0.02
	6.5021		0.54 0.08	0.42 0.05	0.47 0.02	0.49 0.01
19307+2758	6.4995			2.64 0.19	3.47 0.26	
19553–0644	6.4996		1.22 0.10	1.18 0.12	1.10 0.10	1.16 0.06
	7.6001		0.28 0.06	0.88 0.12	1.00 0.11	1.15 0.13
20035+3601	6.4997		0.79 0.04	0.76 0.02	0.75 0.01	0.74 0.01
20181+4044	6.4970		2.72 0.07	2.29 0.04	2.31 0.02	2.31 0.01
20203+3924	6.4970		2.07 0.22	1.96 0.18	2.01 0.22	1.68 0.19
20375+1436	6.4942		1.25 0.14	0.89 0.11	0.93 0.11	1.07 0.14
	6.4998		0.84 0.05	0.97 0.06	1.03 0.08	0.83 0.09
21044–1951	6.4998		2.67 0.26	2.18 0.22	2.03 0.21	1.72 0.18
21145+1000	6.4944		0.19 0.04	0.09 0.04	0.09 0.04	0.43 0.05
21148+3803	6.4944		2.80 0.22	2.74 0.12	2.62 0.09	2.59 0.10
21186+1134	6.4999		1.68 0.18	1.62 0.14	1.53 0.17	1.57 0.14
21441+2845	6.7811		1.47 0.03		1.41 0.02	1.38 0.01
21501+1717	6.4945		1.21 0.14	1.25 0.09	1.11 0.09	1.08 0.06
22300+0426	6.4945		2.01 0.22	1.78 0.20	1.54 0.15	1.42 0.12
22586+0921	6.4972		0.22 0.04	1.62 0.19	0.50 0.08	–0.39 0.83

Table 3. Literature Δm Values

WDS or α, δ (2000)	Hipparcos Δm	Mean WDS Δm	Δm Catalog Δm
00022+2705		3.60±1.19	3.04
00318+5431	0.04±0.01	0.25 0.17	
02140+4729	0.66 0.01	0.72 0.21	0.57±0.09
04139+0916	2.25 0.04	2.68 0.48	2.18
04239+0928		0.07 0.09	
04301+1538	2.52 0.03	2.42 0.54	2.38 0.06
04382–1418	2.90 0.02	2.99 0.34	3.43
04512+1104	0.24 0.20	0.12 0.23	0.19
05387–0236	1.21 0.05	1.15 0.53	
05413+1632	1.51 0.04	0.65 0.38	2.0
06573+5825		1.19 0.48	1.20
09006+4147	2.30 0.04	2.14 0.35	1.83 0.08
11182+3132		0.53 0.24	0.48 0.03
13099–0532	2.34 0.04		
13100+1732		0.05 0.08	0.41 0.51
14411+1344	0.05 0.01	0.52 0.59	0.04 0.03
15038+4739	0.78 0.02	0.78 0.27	0.79 0.15
15183+2650	0.05 0.01	0.27 0.20	0.04 0.01
15232+3017	0.29 0.01	0.38 0.20	0.25 0.06
15427+2618	1.56 0.01	2.34 0.68	1.48 0.07
16309+0159	1.04 0.02	1.37 0.54	1.01 0.03
17104–1544	0.51 0.01	0.46 0.21	0.5
19307+2758	2.12 0.02	1.97 0.41	
19553–0644	1.04 0.05	0.99 0.35	
20035+3601	0.61 0.01	0.50 0.17	0.52 0.00
20181+4044	2.27 0.02	2.10 0.27	2.25 0.17
20203+3924		1.81 0.55	
20375+1436	0.91 0.05	0.91 0.34	0.9 0.3
21044–1951	2.37 0.06	1.60 0.43	1.67 0.72
21145+1000	0.33 0.32	0.16 0.19	0.62 0.31
21148+3803	2.89 0.03	3.13 0.79	2.46 0.15
21186+1134	1.57 0.25	1.69 0.38	1.13 0.46
21441+2845	1.45 0.01	1.44 0.29	1.47 0.21
21501+1717	1.21 0.31	1.06 0.48	1.1
22300+0426	1.54 0.01	1.40 0.35	1.33 0.12
22586+0921		0.24 0.19	0.7

^aRed Δm from SOR AO paper is 1.04±0.01.

NOTES TO TABLE 7

- a Object went beyond LC III table, used supergiant table instead.
- b Used LC I table.
- c Used WDS spectral type.
- d No Hipparcos measurement.
- e Our type not consistent with WDS.
- f Inconsistent result, used WDS type instead.
- g Edwards (1976)
- h Christie & Walker (1969)

Table 4. Component Apparent Magnitudes

WDS α, δ (2000)	B		V		R		I	
	Prim	Sec	Prim	Sec	Prim	Sec	Prim	Sec
00022+2705			5.81±0.03	8.89±0.29	5.25±0.03	7.95±0.27	4.85±0.03	7.20±0.26
00318+5431			5.41 0.03	5.56 0.05	5.43 0.03	5.53 0.05	5.54 0.03	5.67 0.05
02140+4729			6.54 0.03	7.19 0.07	6.18 0.02	6.77 0.05	5.95 0.02	6.49 0.03
04139+0916			4.95 0.02	7.38 0.04	4.26 0.02	7.12 0.07	3.78 0.02	7.06 0.13
04239+0928			5.51 0.04	6.41 0.13	5.39 0.04	6.36 0.12	5.62 0.03	5.83 0.05
04301+1538			5.70 0.03	8.05 0.20	5.40 0.03	7.59 0.17	5.23 0.03	7.25 0.12
			5.68 0.02	8.22 0.07	5.38 0.02	7.75 0.05	5.20 0.02	7.41 0.04
04382–1418					3.14 0.03	5.53 0.23	2.54 0.02	5.56 0.20
04512+1104			7.45 0.03	7.60 0.05	6.98 0.03	7.16 0.05	6.67 0.03	6.87 0.05
05387–0236			4.10 0.03	5.34 0.10	4.15 0.04	5.49 0.13	4.41 0.04	5.66 0.16
05413+1632			5.11 0.04	6.58 0.16	5.11 0.04	6.62 0.18	5.23 0.04	6.75 0.18
06573+5825			4.67 0.03	5.83 0.12	3.96 0.03	5.37 0.08	3.48 0.04	5.08 0.18
09006+4147			4.07 0.03	6.62 0.27	3.71 0.03	5.90 0.15	3.50 0.04	5.56 0.23
11182+3132	4.87±0.04	5.49±0.09	4.31 0.04	4.84 0.10	3.79 0.03	4.26 0.07	3.48 0.03	3.88 0.05
	4.92 0.03	5.39 0.06	4.35 0.03	4.77 0.07	3.87 0.03	4.15 0.07	3.58 0.03	3.76 0.05
13099–0532	4.54 0.04	6.65 0.23	4.52 0.03	6.73 0.20	4.48* 0.13	6.56* 0.24	4.11* 0.32	6.27* 0.38
13100+1732	5.50 0.03	5.54 0.05	5.08 0.04	5.07 0.07	4.83* 0.11	4.83* 0.12	4.21* 0.25	4.21* 0.25
14411+1344	4.58 0.02	4.58 0.03	4.52 0.02	4.54 0.02	4.51 0.02	4.52 0.02	4.51 0.02	4.53 0.02
	4.59 0.05	4.57 0.10	4.50 0.03	4.57 0.05	4.51 0.02	4.52 0.04	4.50 0.02	4.55 0.04
15038+4739	5.71 0.04	6.99 0.17	5.19 0.03	6.01 0.08	4.38* 0.14	4.99* 0.14	4.51* 0.32	5.03* 0.32
15183+2650	7.79 0.03	7.81 0.05	7.34 0.02	7.35 0.04				
15232+3017	6.16 0.02	6.48 0.03	5.60 0.02	5.88 0.03	5.13 0.02	5.39 0.02	4.85 0.02	5.10 0.02
	7.64 0.03	8.00 0.07	7.21 0.03	7.50 0.07				
15427+2618	4.05 0.02	5.74 0.08	4.08 0.02	5.64 0.03	4.14 0.02	5.57 0.03	4.18 0.02	5.51 0.04
	4.02 0.03	5.87 0.11	4.08 0.03	5.67 0.12	4.14 0.02	5.55 0.06	4.19 0.02	5.47 0.06
16309+0159			4.17 0.04	5.24 0.15	4.20 0.02	5.23 0.05	4.21 0.02	5.23 0.04
	4.17 0.03	5.29 0.08	4.16 0.02	5.27 0.06	4.18 0.02	5.27 0.06	4.20 0.02	5.26 0.04
17104–1544	3.00 0.03	3.50 0.07	2.94 0.03	3.46 0.05	2.91 0.02	3.44 0.04	2.90 0.02	3.43 0.03
	2.99 0.04	3.53 0.09	2.98 0.03	3.40 0.06	2.93 0.02	3.40 0.03	2.91 0.02	3.40 0.02
19307+2758			3.18 0.03	5.82 0.19	2.26 0.02	5.73 0.26		
19553–0644	7.20 0.03	8.42 0.10	6.82 0.04	8.00 0.13	6.60* 0.14	7.70* 0.17	5.47* 0.32	6.63* 0.33
	7.51 0.03	7.79 0.07	6.90 0.04	7.78 0.13	6.62* 0.14	7.62* 0.18	5.47* 0.32	6.62* 0.35
20035+3601	7.16 0.02	7.95 0.05	7.07 0.02	7.83 0.03	6.95 0.02	7.70 0.02	6.84 0.02	7.58 0.02
20181+4044	6.03 0.02	8.75 0.07	5.96 0.02	8.25 0.04	5.81 0.02	8.12 0.03	5.80 0.02	8.11 0.02
20203+3924	6.44 0.03	8.51 0.22	6.40 0.03	8.36 0.18	6.33 0.04	8.34 0.22	6.35 0.04	8.03 0.19
20375+1436	4.37 0.04	5.62 0.15	4.03 0.04	4.92 0.12	3.61 0.04	4.54 0.12	3.33 0.04	4.40 0.15
	4.48 0.03	5.32 0.06	4.00 0.03	4.97 0.07	3.59 0.03	4.62 0.09	3.41 0.03	4.24 0.10
21044–1951	5.11 0.03	7.78 0.26	4.98 0.03	7.16 0.22	4.84 0.03	6.87 0.21	4.81 0.04	6.53 0.18
21145+1000	5.65 0.03	5.84 0.05	5.20 0.03	5.29 0.05	4.77 0.03	4.86 0.05	4.34 0.03	4.77 0.06
21148+3803	4.21 0.03	7.01 0.22	3.81 0.02	6.55 0.12	3.47 0.02	6.09 0.09	3.24 0.02	5.83 0.10
21186+1134	7.31 0.04	8.99 0.18	7.25 0.03	8.87 0.14	6.97* 0.13	8.50* 0.22	5.12* 0.25	6.69* 0.29
21441+2845	5.25 0.02	6.72 0.04			4.39 0.02	5.80 0.03	4.12 0.02	5.50 0.02
22300+0426	6.05 0.04	8.06 0.22	5.71 0.04	7.49 0.20	5.45 0.04	6.99 0.15	5.27 0.03	6.69 0.12

Table 5. Component Colors

WDS α, δ (2000)	B–V				V–R				V–I			
	Prim		Sec		Prim		Sec		Prim		Sec	
00022+2705					0.57±0.04		0.95±0.40		0.96±0.04		1.69±0.39	
00318+5431					–0.02	0.04	0.03	0.07	–0.13	0.04	–0.11	0.07
02140+4729					0.36	0.04	0.42	0.08	0.59	0.04	0.70	0.07
04139+0916					0.69	0.03	0.26	0.09	1.17	0.03	0.32	0.14
04239+0928					0.12	0.06	0.05	0.17	–0.11	0.05	0.58	0.14
04301+1538					0.30	0.04	0.46	0.27	0.47	0.04	0.80	0.24
					0.30	0.03	0.47	0.09	0.48	0.03	0.81	0.08
04512+1104					0.47	0.04	0.44	0.07	0.78	0.04	0.73	0.07
05387–0236					–0.05	0.05	–0.15	0.17	–0.31	0.05	–0.32	0.19
05413+1632					–0.00	0.06	–0.04	0.25	–0.12	0.06	–0.17	0.25
06573+5825					0.71	0.04	0.46	0.14	1.19	0.05	0.75	0.22
09006+4147					0.36	0.04	0.72	0.31	0.57	0.05	1.06	0.36
11182+3132	0.56±0.05		0.65±0.13		0.52	0.05	0.58	0.12	0.83	0.05	0.96	0.11
	0.57	0.04	0.62	0.09	0.48	0.05	0.62	0.10	0.78	0.04	1.02	0.08
13099–0532	0.01	0.05	–0.09	0.31	0.04	0.14	0.17	0.31	0.41	0.32	0.46	0.43
13100+1732	0.43	0.05	0.48	0.09	0.25	0.12	0.24	0.14	0.87	0.25	0.86	0.26
14411+1344	0.06	0.03	0.04	0.04	0.02	0.03	0.03	0.03	0.01	0.03	0.01	0.03
	0.09	0.06	0.00	0.11	–0.01	0.04	0.05	0.06	0.00	0.04	0.02	0.06
15038+4739	0.52	0.05	0.98	0.18	0.81	0.14	1.02	0.16	0.67	0.32	0.97	0.33
15183+2650	0.46	0.04	0.47	0.06								
15232+3017	0.56	0.03	0.60	0.04	0.47	0.03	0.49	0.04	0.75	0.03	0.78	0.04
	0.43	0.05	0.50	0.10								
15427+2618	–0.03	0.03	0.10	0.09	–0.06	0.03	0.07	0.04	–0.10	0.03	0.13	0.05
	–0.05	0.04	0.21	0.17	–0.07	0.04	0.11	0.14	–0.12	0.04	0.19	0.14
16309+0159					–0.02	0.05	0.02	0.15	–0.03	0.05	0.02	0.15
	0.01	0.04	0.02	0.09	–0.02	0.03	0.00	0.08	–0.03	0.03	0.02	0.07
17104–1544	0.06	0.04	0.04	0.08	0.03	0.03	0.02	0.06	0.04	0.03	0.03	0.06
	0.00	0.05	0.12	0.10	0.05	0.04	–0.00	0.06	0.07	0.03	–0.00	0.06
19307+2758					0.92	0.03	0.09	0.32				
19553–0644	0.38	0.05	0.42	0.16	0.22	0.15	0.30	0.21	1.34	0.32	1.36	0.35
	0.61	0.05	0.01	0.14	0.28	0.15	0.16	0.22	1.43	0.32	1.16	0.37
20035+3601	0.09	0.03	0.12	0.05	0.12	0.03	0.13	0.04	0.22	0.03	0.24	0.04
20181+4044	0.06	0.03	0.49	0.09	0.15	0.03	0.13	0.05	0.16	0.03	0.14	0.05
20203+3924	0.05	0.05	0.16	0.29	0.07	0.05	0.02	0.29	0.05	0.05	0.33	0.27
20375+1436	0.34	0.06	0.70	0.19	0.41	0.05	0.37	0.16	0.69	0.06	0.51	0.19
	0.48	0.04	0.35	0.09	0.42	0.04	0.36	0.11	0.60	0.04	0.74	0.12
21044–1951	0.13	0.04	0.62	0.34	0.14	0.05	0.29	0.31	0.16	0.05	0.62	0.29
21145+1000	0.45	0.04	0.55	0.07	0.43	0.04	0.43	0.07	0.86	0.04	0.52	0.08
21148+3803	0.40	0.03	0.46	0.25	0.34	0.03	0.46	0.15	0.58	0.03	0.73	0.16
21186+1134	0.06	0.05	0.12	0.23	0.28	0.14	0.37	0.26	2.13	0.25	2.18	0.32
22300+0426	0.34	0.05	0.57	0.30	0.27	0.05	0.51	0.26	0.44	0.05	0.80	0.24

Table 6. Component Absolute Magnitudes

WDS α, δ (2000)	B				V				R				I			
	Prim		Sec		Prim		Sec		Prim		Sec		Prim		Sec	
00022+2705					5.34±0.09		8.42±0.30		4.78±0.09		7.48±0.28		4.3 8±0.09		6.73±0.27	
00318+5431					0.23	0.25	0.38	0.26	0.25	0.25	0.35	0.26	0.36	0.25	0.49	0.26
02140+4729					3.45	0.09	4.10	0.11	3.09	0.09	3.68	0.10	2.86	0.09	3.40	0.09
04139+0916					-0.33	0.34	2.10	0.35	-1.02	0.34	1.84	0.35	-1.50	0.34	1.78	0.37
04239+0928					0.09	0.25	0.99	0.28	-0.03	0.25	0.94	0.28	0.20	0.25	0.41	0.25
04301+1538					2.50	0.12	4.85	0.23	2.20	0.12	4.39	0.21	2.03	0.12	4.05	0.17
					2.48	0.12	5.02	0.14	2.18	0.12	4.55	0.13	2.00	0.12	4.21	0.12
04382-1418									0.51	0.05	2.90	0.23	-0.09	0.05	2.93	0.21
04512+1104					3.97	0.13	4.12	0.13	3.50	0.13	3.68	0.13	3.19	0.13	3.39	0.13
05387-0236					-3.63	0.70	-2.39	0.70	-3.58	0.70	-2.24	0.71	-3.32	0.70	-2.07	0.71
05413+1632					-1.69	0.61	-0.22	0.63	-1.69	0.61	-0.18	0.64	-1.57	0.61	-0.05	0.64
06573+5825					1.08	0.09	2.24	0.15	0.37	0.09	1.78	0.12	-0.11	0.10	1.49	0.20
09006+4147					2.99	0.06	5.54	0.27	2.63	0.06	4.82	0.16	2.42	0.06	4.48	0.23
11182+3132	3.79±0.06		4.41±0.10		3.23	0.06	3.76	0.11	2.71	0.06	3.18	0.08	2.40	0.06	2.80	0.07
13099-0532	-0.98	0.31	1.13	0.38	-1.00	0.31	1.21	0.37	-1.04	0.33	1.04	0.39	-1.41	0.44	0.75	0.49
13100+1732	4.72	0.86	4.76	0.86	4.30	0.86	4.29	0.86	4.05	0.86	4.05	0.87	3.43	0.89	3.43	0.89
14411+1344	0.86	0.15	0.86	0.15	0.80	0.15	0.82	0.15	0.79	0.15	0.80	0.15	0.79	0.15	0.81	0.15
	0.87	0.16	0.85	0.18	0.78	0.15	0.85	0.16	0.79	0.15	0.80	0.15	0.78	0.15	0.83	0.15
15038+4739	5.18	0.05	6.46	0.17	4.66	0.04	5.48	0.08	3.85	0.14	4.46	0.14	3.98	0.32	4.50	0.32
15183+2650	4.87	0.11	4.89	0.12	4.42	0.11	4.43	0.11								
15232+3017	4.81	0.05	5.13	0.06	4.25	0.05	4.53	0.06	3.78	0.05	4.04	0.05	3.50	0.05	3.75	0.05
	6.29	0.06	6.65	0.09	5.86	0.06	6.15	0.09								
15427+2618	0.81	0.07	2.50	0.10	0.84	0.07	2.40	0.07	0.90	0.07	2.33	0.07	0.94	0.07	2.27	0.08
	0.78	0.07	2.63	0.13	0.84	0.07	2.43	0.14	0.90	0.07	2.31	0.09	0.95	0.07	2.23	0.09
16309+0159					0.63	0.15	1.70	0.21	0.66	0.15	1.69	0.16	0.67	0.15	1.69	0.15
	0.63	0.15	1.75	0.17	0.62	0.15	1.73	0.16	0.64	0.15	1.73	0.16	0.66	0.15	1.72	0.15
17104-1544	0.94	0.06	1.44	0.08	0.88	0.06	1.40	0.07	0.85	0.05	1.38	0.06	0.84	0.05	1.37	0.06
	0.93	0.06	1.47	0.10	0.92	0.06	1.34	0.08	0.87	0.05	1.34	0.06	0.85	0.05	1.34	0.05
19307+2758					-2.18	0.15	0.46	0.24	-3.10	0.15	0.37	0.30				
19553-0644	2.54	0.22	3.76	0.24	2.16	0.22	3.34	0.26	1.94	0.26	3.04	0.28	0.81	0.39	1.97	0.40
	2.85	0.22	3.13	0.23	2.24	0.22	3.12	0.26	1.96	0.26	2.96	0.28	0.81	0.39	1.96	0.41
20181+4044	-2.36	0.63	0.36	0.63	-2.43	0.63	-0.14	0.63	-2.58	0.63	-0.27	0.63	-2.59	0.63	-0.28	0.63
20203+3924	1.25	0.20	3.32	0.29	1.21	0.20	3.17	0.27	1.14	0.20	3.15	0.29	1.16	0.20	2.84	0.27
20375+1436	1.99	0.07	3.24	0.16	1.65	0.07	2.54	0.13	1.23	0.07	2.16	0.13	0.95	0.07	2.02	0.16
	2.10	0.06	2.94	0.08	1.62	0.06	2.59	0.09	1.21	0.06	2.24	0.11	1.03	0.06	1.86	0.12
21044-1951	1.68	0.16	4.35	0.30	1.55	0.16	3.73	0.27	1.41	0.16	3.44	0.26	1.38	0.16	3.10	0.24
21145+1000	4.32	0.05	4.51	0.06	3.87	0.05	3.96	0.06	3.44	0.05	3.53	0.06	3.01	0.05	3.44	0.07
21148+3803	2.61	0.04	5.41	0.22	2.21	0.03	4.95	0.12	1.87	0.03	4.49	0.09	1.64	0.03	4.23	0.10
21186+1134	3.79	0.14	5.47	0.22	3.73	0.13	5.35	0.19	3.45	0.18	4.98	0.26	1.60	0.28	3.17	0.32
21441+2845	3.50	0.04	4.97	0.05					2.64	0.04	4.05	0.05	2.37	0.04	3.75	0.04
22300+0426	2.55	0.14	4.56	0.26	2.21	0.14	3.99	0.24	1.95	0.14	3.49	0.20	1.77	0.14	3.19	0.18

Table 7. Newly Determined Spectral Types

WDS or α, δ (2000)	WDS Type	Other Type	B-V Type	V-R Type	V-I Type	V_{abs} Type	Assigned
00022+2705	G2V	G2V+K6V g G3V+K7V h		G7(3-9) K5(4-5)	G8(6-9) K5(4-8)	G7(6-7) K8(7-M0)	G7(6-8) K5(4-6)
00318+5431	B9V	B7.5V+B8.5V g		B9(7-A0) A0(B7-A3)	B8(7-9) B8(B6-A1)	B8(6-A0) B9(9-A0)	B8(7-9) B9(B8-A0)
02140+4729	F4V	F3V+F6V g F1V+F4V h		F2(0-8) F6(3-G0)	F2(0-5) F6(5-9)	F2(1-2) F8(8-9)	F2(1-3) F7(6-8)
04139+0916	G5III*+A7V			G5(4-8) A8(6-F2)	G5(4-8) A8(4-F0)	K7(4-M3) A6(4-9)	G5(4-8) A8(5-F0)
04239+0928	A3V	A3V+A4V h		A3(2-6) A1(B0-F0)	B8(7-9) F3(A9-F7)	B9(3-A0) A1(0-2)	A0(B7-A4) A1(B5-F5)
04301+1538	F0V*	A8V+G2V g		F0(A9-F1) F7(4-9)	F0(A9-F1) G0(F7-G5)	A9(6-F0) G7(6-8)	F0(A9-F1) G0(F7-G7)
04512+1104	F7V+F7V	F7V+F7V g F8V+F8V h	F7(4-G0)	F8(6-G0) F7(6-9)	F8(7-G0) F8(7-9)	F8(8-8) F7(6-8)	F8(7-G0) F8(7-G0)
05387-0236	O9.5V	O9V+B0.5V g		B6(2-9) O9(5-A0)	B2(1-3) B2(O4-B5)	B0(O9-B1) B2(1-3)	B3(1-4) B2(O9-B4)
05413+1632	B3IV	B3IV+B3V g B3V+B4V h		B9(6-A1) B7(O5-A7)	B8(7-9) B7(O-A2)	B3(2-5) B8(6-9)	B8(7-9) B7(2-9)
06573+5825 a	G5III			G8(0-K0) F8(5-G2)	G8(0-K0) F8(4-G2)	A7(6-8) OffScale	G8(0-K0) F8(5-G2)
09006+4147	F5V			F3(1-5) K2(F5-K5)	F3(1-4) K0(F7-K4)	F1(0-1) G9(6-K0)	F3(1-4) K0(F8-K4)
11182+3132	G0V+G0V		F9(F8-G0) G2(F7-G7)	F8(F6-G0) G9(2-K1)	F9(F8-G0) G9(8-K0)	F1(0-2) F7(6-8)	F9(F8-G0) G9(6-K1)
13099-0532	AIV		A0(0-1) B8(7-9)	A1(B2-F0) A6(O9.5-F8)	A9(A2-F7) F0(A0-G0)	B6(5-7) B6(5-7)	A0(B9-A1) B8(7-9)
13100+1732	F6V	F5V+F5V g	F5(3-6) F6(4-9)	A8(A4-F3) A8(A3-F4)	G3(F4-K1) G3(F4-K1)	G0(F5-G6) G0(F6-G6)	F5(3-6) F6(4-9)
14411+1344	A2V	A2III+A2III g	A2(1-3) A1(0-3)	A0(B9-A1) A0(B9-A1)	A0(0-1) A0(0-1)	A0(0-0) A0(0-0)	A0(B9-A1) A0(B9-A1)
15038+4739	G0V		F7(6-9) K3(0-5)	K3(1-5) K5(4-7)	F6(A8-G8) G8(F0-K3)	G2(2-2) G8(4-9)	F7(6-9) K4(2-6)
15183+2650	G0V		F6(5-7) F6(5-7)			G0(F9-G1) G0(F9-G1)	F6(5-7) F6(5-7)
15232+3017	G3V	G1V+G3V g	F9(8-G0) G0(F9-G3)	F8(A9-F1) G0(F7-G2)	F8(7-8) F9(8-G0)	F9(9-G0) G1(0-2)	F8(7-9) G0(F9-G1)
15427+2618	B9IV+A3V	B9IV+A3V g	B9(9-A0) A3(0-7)	B6(2-8) A2(0-4)	B8(8-9) A3(2-4)	A1(0-1) A8(7-F0)	B9(8-A0) A3(2-4)
16309+0159	A0V+A4V	A0V+A4V g	A0(0-1) A1(B9-A4)	B8(6-9) B9(3-A2)	A0(B9-0) A0(B9-A2)	A0(0-0) A4(3-5)	A0(B9-A0) A0(B8-A2)
17104-1544	A2IV	A1V+A3V g	A2(1-3) A1(B9-A4)	A0(B9-A1) A0(B7-A2)	A1(0-2) A1(A0-A2)	A1(1-1) A2(2-3)	A1(0-2) A1(0-2)
19307+2758 b,c	K3II+B0V			K3(3-3) A2(O5-F5)		OffScale A0(B9-A1)	K3(3-3) B0(0-0)
20035+3601 d	O9.5III		A3(2-4) A2(1-3)	A4(2-5) A5(3-7)	A5(4-6) A6(3-7)		A4(3-5) A4(2-6)
20181+4044 e	O9V		A2(1-3) F7(4-G0)	A5(3-7) A4(2-7)	A4(2-5) A3(2-4)	B2(1-3) B8(7-A0)	A4(2-6) A3(2-7)
20203+1436	A0IV	A1V+F6V g A0V+F1V h	A2(0-4) A6(B7-F5)	A2(0-4) A0(O-F1)	A1(0-2) A9(1-F3)	A2(1-3) F1(0-2)	A2(1-3) A5(B7-F3)
20375+1436	F5IV	F5III+F5IV g F6III+F6IV h	F6(5-6) F2(A9-F5)	F6(4-8) F2(A9-F8)	F4(3-5) F7(4-G2)	A4(3-5) A9(8-F0)	F5(4-6) F2(A9-F4)
21044-1951	A5V		A5(3-6) G1(F0-K3)	A4(2-7) F0(B8-G8)	A4(2-5) F4(A8-G5)	A3(2-4) F2(1-8)	A4(3-5) F2(A5-G0)
21145+1000	F5V+G0V	F7V+F7V h	F5(4-6) F9(7-G2)	F6(5-8) F6(2-G0)	G2(0-5) F1(0-3)	F6(5-7) F8(7-8)	F6(5-7) F6(2-G0)
21148+3803	F3IV-V	F0IV+G1V g F2IV+G0V h	F4(2-5) F6(A8-G1)	F2(0-3) F8(0-G9)	F3(2-4) F7(2-G5)	A7(5-8) G4(2-5)	F3(2-4) F7(2-G0)
21186+1134 f	G0V	F7V+G6V h	A2(0-5) A4(B7-F2)	F0(A4-F6) F3(A3-K0)	M0(K6-M1) M0(K6-M1)	F7(5-8) G6(5-8)	G0(F0-M0) G6(A5-M0)

Table 8. Effective Temperatures, Bolometric Magnitudes, and Masses

WDS or α, δ (2000)	Assigned Type	T_{eff}	M_{bol}	Orbital Mass Sum \mathcal{M}_{\odot}	Spectroscopic Mass Sum \mathcal{M}_{\odot}
00022+2705	G7(6-8)	5637±70	5.00±0.11	1.49±0.09	1.6
	K5(4-6)	4350 200	7.70 0.32		
00318+5431	B8(7-9)	11900 750	−0.57 0.29	n/a	8.0
	B9(B8-A0)	10500 750	−0.13 0.28		
02140+4729	F2(1-3)	6890 100	3.34 0.09	2.39 0.26	2.7
	F7(6-8)	6280 70	3.95 0.11		
04139+0916	G5(4-8)	5150 100	−0.67 0.34	n/a	5.0
	A8(5-F0)	7580 300	2.00 0.35		
04239+0928	A0(B7-A4)	9520 1200	−0.21 0.33	4.68	6.2
	A1(B5-F5)	9230 2240	0.76 0.46		
04301+1538	F0(A9-F1)	7200 150	2.39 0.12	2.56	2.8
	G0(F7-G7)	5850 600	4.82 0.17		
04512+1104	F8(7-G0)	6200 40	3.81 0.13	3.04 0.49	2.4
	F7(6-8)	6280 40	3.97 0.13		
05387-0236	B3(1-4)	18700 1500	−5.57 0.73	n/a	21*
	B2(O9-B4)	22000 4000	−4.74 0.81		
05413+1632	B8(7-9)	11900 625	−2.20 0.62	n/a	9.1
	B7(2-9)	13000 2800	−1.24 0.77		
06573+5825	G8(O-K0)	4900 275	0.66 0.11	3.65 1.83	4.1
	F8(5-G2)	6100 400	2.15 0.16		
09006+4147	F3(1-4)	6740 100	2.87 0.06	2.42 0.12	2.2
	K0(F8-K4)	5250 400	5.23 0.29		
11182+3132	F9(F8-G0)	6220 43	3.06 0.06	2.21	1.9
	G9(6-K1)	5410 110	3.40 0.11		
13099-0532	A0(B9-A1)	9520 317	−1.30 0.32	n/a	7.5
	B8(7-9)	11900 650	0.41 0.39		
13100+1732	F5(3-6)	6440 86	4.16 0.86	2.54 0.20	2.5
	F6(4-9)	6378 140	4.14 0.86		
14411+1344	A0(B9-A1)	10100 380	0.40 0.18	2.34	n/a
	A0(B9-A1)	10100 380	0.40 0.18		
15038+4739	F7(6-9)	6280 60	4.51 0.04	2.70 0.16	1.9*
	K4(2-6)	4590 95	4.76 0.14		
15183+2650	F6(5-7)	6360 40	4.27 0.11	2.53 0.33	2.5*
	F6(5-7)	6360 40	4.28 0.11		
15232+3017	F8(7-9)	6200 40	4.09 0.05	2.43	2.3
	G0(F9-G1)	6030 43	4.35 0.06		
15427+2618	B9(8-A0)	10500 245	0.33 0.14	4.23 0.55	6.2
	A3(2-4)	8720 120	2.23 0.07		
16309+0159	A0(B9-A0)	9520 70	0.32 0.15	7.15	6.5
	A0(B8-A2)	9520 730	1.43 0.22		
17104-1544	A1(0-2)	9230 130	0.65 0.26	4.81 3.31	5.5
	A1(0-2)	9230 130	0.65 0.26		
19307+2758	K3(3-3)	4080 10	−2.93 0.15	n/a	23
	B0(0-0)	30000 100	−2.70 0.24		
20035+3601	A4(3-5)	8460 130		n/a	n/a*
	A4(2-6)	8460 250			
20181+4044	A4(2-6)	8460 250	−2.59 0.63	n/a	n/a*
	A3(2-7)	8720 280	−0.31 0.63		
20203+1436	A2(1-3)	8970 120	1.01 0.20	1.56	4.8
	A5(B7-F3)	8200 1700	−0.29 0.67		
20375+1436	F5(4-6)	6440 60	1.48 0.06	3.34 0.27	3.8
	F2(A9-F4)	6890 370	2.48 0.09		
21044-1951	A4(3-5)	8460 130	1.39 0.16	2.87 0.75	3.8
	F2(A5-G0)	6890 540	3.62 0.27		
21145+1000	F6(5-7)	6360 40	3.72 0.05	2.35 0.12	2.5
	F6(2-G0)	6360 215	3.81 0.06		
21148+3803	F3(2-4)	6740 75	2.09 0.03	2.71 0.11	2.7
	F7(2-G0)	6280 210	4.80 0.12		
21186+1134	G0(F0-M0)	6030 840	3.55 0.35	3.07 0.55	2.0*
	G6(A5-M0)	5703 1090	5.08 0.36		